5 (2023) 100016

Contents lists available at ScienceDirect

IPEM-Translation

journal homepage: www.elsevier.com/locate/ipemt

Full Length Article

Automated continuous distraction osteogenesis system for limb lengthening and reconstruction

Yiyuan Fu (付益源)[a], Fanwu Meng (孟凡武)[a], Xinghua Yin (尹星华)[b], Jianming Gu (顾建明)[b], Zhuyi Ma (马祝一)[b], Yixin zhou (周一新)[b,*]

[a] School of Mechanical Engineering, Beijing Institute of Technology, Beijing, China
[b] Department of Orthopaedics, Beijing Jishuitan Hospital, Fourth Clinical College of Peking University, Xinjiekou East Street, Xicheng District, Beijing 100035, China

ARTICLE INFO

Keywords:
Automated continuous distractor
Limb lengthening
Distraction osteogenesis
Medical devices

ABSTRACT

Distraction osteogenesis (DO) is a classical surgical technique for limb lengthening and reconstruction (LLR). Most existing DO devices for LLR are operated manually, and the accurate DO process is user dependant, which could affect new bone formation. Recently, automated devices have been introduced for continuous DO processes to aid in tissue healing. To the best of our knowledge, few automated continuous distraction osteogenesis (ACDO) devices have focused on DO surgery for the long bones of the extremities and monitoring of their status during the surgical process. This study presents a novel ACDO device, which is driven by a deceleration stepper motor for further reduction in total mass and amplification in distraction force, including a precise and programmable man–machine-interaction system to allow surgeons to control and monitor the treatment remotely. The mechanical device was verified to be capable of generating a continuous and controllable distraction force and rate. The proposed man–machine-interaction system possesses the functions of customizing and following up on treatment plan by clinicians, including setting the DO process, measuring and displaying parameters, and uploading DO information to the data cloud. During electromechanical system simulation and prototype experiments, the performance of the proposed system was consistent with the setting DO parameters and treatment plan.

1. Introduction

Distraction osteogenesis (DO) is a classical technique for limb lengthening and reconstruction (LLR) that induces bone formation in an expanding skeletal gap [1–5]. While manually operated external DO devices are common tools for LLR surgeons to correct various bone defects or limb length discrepancies, with or without angular deformities [6–8], the treatment can be lengthy and dependant on patient compliance [9]. In addition, manual operations may cause minor vibrations in these devices, as well as inaccurate distraction rates and lengths, which is against the principle of gradual distractions and, subsequently, harmful to bone tissue healing. Automation of DO may minimize these impacts [10]. The key elements of automated continuous DO (ACDO) treatments are the distraction rate (DR), distraction vector (DV), and output distraction force (DF) [11–13].

Various movement mechanisms and actuators have recently been studied and used in the design and development of ACDO devices, including piezo-electric motors [11], motor-based actuators [14], electro-mechanical systems [15–21], hydraulic valves [22–24], spring-mediated systems [25–28], shape memory alloys [28], and load cells [29]. Most ACDO devices are neither portable nor lightweight, making them incapable of meeting the requirements for use. Furthermore, the existing distractors are operated manually with uncertain DR and low stability. The common distractors are manually twisted around, and the movable side can translate by 1 mm, whereas some distractors can subdivide this process into two or four parts, i.e., translations of 0.5 or 0.25 mm. In addition to the high cost, the DF generated by manual operations is not precisely controlled, whereas ACDO produces a high-quality, stable, and smooth continuous DF to facilitate osteogenesis with less irritation of surrounding tissue [30]. Furthermore, the lack of feedback control, human–machine interaction, and automatic measurement in ACDO devices make setting and monitoring the DO process

Abbreviations: ACDO, Automated continuous distraction osteogenesis; BS, Bone segments; CDC, cyclic distraction-compression; DF, Distraction force; DO, Distraction osteogenesis; DR, Distraction rate and rhythm; DV, Distraction vector; LCD, Liquid crystal display; LLR, Limb lengthening and reconstruction.

* Corresponding author.
E-mail address: orthoyixin@yahoo.com (Y. zhou).

https://doi.org/10.1016/j.ipemt.2023.100016

Available online 11 February 2023

difficult for doctors. With the development of computer and communication technologies, digital information can be transferred to any mobile terminal using Bluetooth or Wi-Fi technology. This concept can be applied to a novel ACDO system to facilitate remote control and monitoring of DO by clinicians.

Based on this observation, we propose a composite ACDO system that includes an automated mechanical device and matched control monitoring system that motorizes and automates the DO process. The designed control monitoring system is capable of facilitating diagnosis and re-inspection by doctors for patients undergoing treatment.

2. Materials and methods

The proposed ACDO system includes a mechanical device and control monitoring system. The ACDO mechanical device must be capable of generating a continuous DF, which can separate bone segments (BS) and pull these BS into the position determined according to the specific diagnosis. Some sensors are incorporated into the device to measure the distraction length and distraction rate (DR). The control monitoring system enables doctors to control the ACDO process and access the patients' treatment information easily and intelligently. This information is obtained from smartphones or personal computers using data cloud technology by the monitoring system, and the information is uploaded by the control system. Fig. 1 presents the overall block diagram of the proposed ACDO system.

The integration unit of the power supply and control board (a printed circuit board for controlling a stepper motor), which is named the electric control box (A in Fig. 1) in the proposed system, is separated from the mechanical device to reduce the weight on patients. A rechargeable power supply generates a 5 V DC that meets the motor rating and supplies the ACDO mechanical device and control board. An 8-bit microcontroller (AT89C51), liquid crystal display (LCD), actuator, three buttons, and independent Bluetooth module are integrated into the control board. These control the motor to indirectly manage the ACDO parameters (D in Fig. 1), which are DR, DF, and DV. The relationship between the motor and these parameters can be determined using Eqs. (1)–(3).

$$v_d = n_m I \ (\mathrm{mm/min}), \tag{1}$$

$$x_d = n_m I t \ (\mathrm{mm}), \tag{2}$$

$$F_a = \frac{T_a 2\pi\eta}{I} \ (\mathrm{N}), \tag{3}$$

where n_m (r/min) is the output rotation speed of the motor, I (mm) is the screw pitch of the lead screw, t (min) is the running time, T_a (N·m) is the output torque of the motor, η is the working efficiency of the lead screw, v_d (mm/min) is the DR, x_d (mm) is the distraction length, and F_a (N) is the DF.

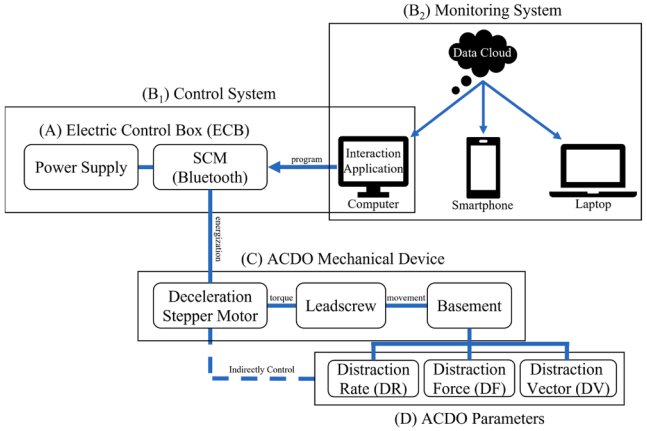

Fig. 1. Block diagram of the proposed ACDO system.

Fig. 2 illustrates the detailed circuit design of the control board. The microcontroller includes 40 digital pins, including VCC (power supply), GND (ground), 24 bidirectional I/O pins, and RST (reset), and operates at a crystal oscillator frequency of 12 MHz. The 16 × 2 LCD LM016L with controller HD44780 is connected to the microcontroller to display the current parameters of the motor. Three buttons are used within the control board to toggle the displayed parameters, as well as start and stop the treatment. The actuator ULN2003A is used to amplify the current driving the motor. The Bluetooth module transfers specific parameters to terminals, such as smartphones or personal computers, for information acquisition for patients or doctors to access, and the terminals upload this information to a data cloud using Wi-Fi.

The control board, terminals, and data cloud are mutually connected to compose the control monitoring system (B in Fig. 1). Owing to the difficulty in reprogramming the microcontrollers, a man–machine-interaction software is designed for doctors to customize the treatment program for patients — this software was programmed using C# language through Visual Studio 2019. The software converts diagnoses written in natural language into a specific C program by obtaining input parameters from the keyboard and calculating the corresponding energization parameters that determine the working conditions of the motor. The ACDO parameters depend on the characteristics of the ACDO mechanical device (C in Fig. 1) (e.g., rotation speed, running time, and output torque of the motor), which can be controlled by the duration and interval of the microcontroller energization. The relationship between the parameters and energizations is described as,

$$t_d = \frac{500\alpha I i}{3v} \ (\mathrm{ms}), \tag{4}$$

where t_d (ms) is the delay time that determines the duration and interval of energization, v (mm/min) is the distraction rate (DR), I (mm) is the pitch of the lead screw, i is the reduction ratio of the motor, and α (°) is the step angle. By modifying the specific parameters in the control program template, the software can generate different control program to implement different t_d by changing the cycle times of machine cycle of the microcontroller (1/12Mhz, 0.083μs). This enables control of the distraction process.

Following assessment, clinicians begin treatment by setting the ACDO parameters using the software, and the control program can be automatically generated and programmed into the microcontroller via a cable. After surgery, patients may choose to be hospitalized or take the device home. A data cloud is set up to save the related patient information. The terminals that obtain digital information from the control board using the Bluetooth module are capable of uploading this information to the data cloud using a mobile network or Wi-Fi, and the doctor can access this data to monitor their patients remotely. The access to the data cloud was tested on an Android emulator in a computer.

In order to generate a continuous DF and transmit a precise linear DV, the mechanical device needs to contain transmission, guiding, and connection sections, and a basement for fixing bone screws and a driver. The transmission section and motor are the main actuators that are vital to the ACDO process, whereas the guiding section, connection section, and basement are auxiliary parts for stabilizing the ACDO process. The different sections work simultaneously and perform different functions for generating a continuous DF and running at a specific DR to separate the BS smoothly and harmlessly. Fig. 3 shows a schematic of the proposed ACDO mechanical device.

A leadscrew mechanism can convert the rotation of a screw into the translation of a nut, which creates a strong linear relationship between the rotary speed and translational velocity. The application of a small torque via the screw–nut mechanism gives rise to a stable and precise linear movement, and, in turn, the generation of large distraction force. With the rotation of the lead screw (3), the traction flange (4) connected

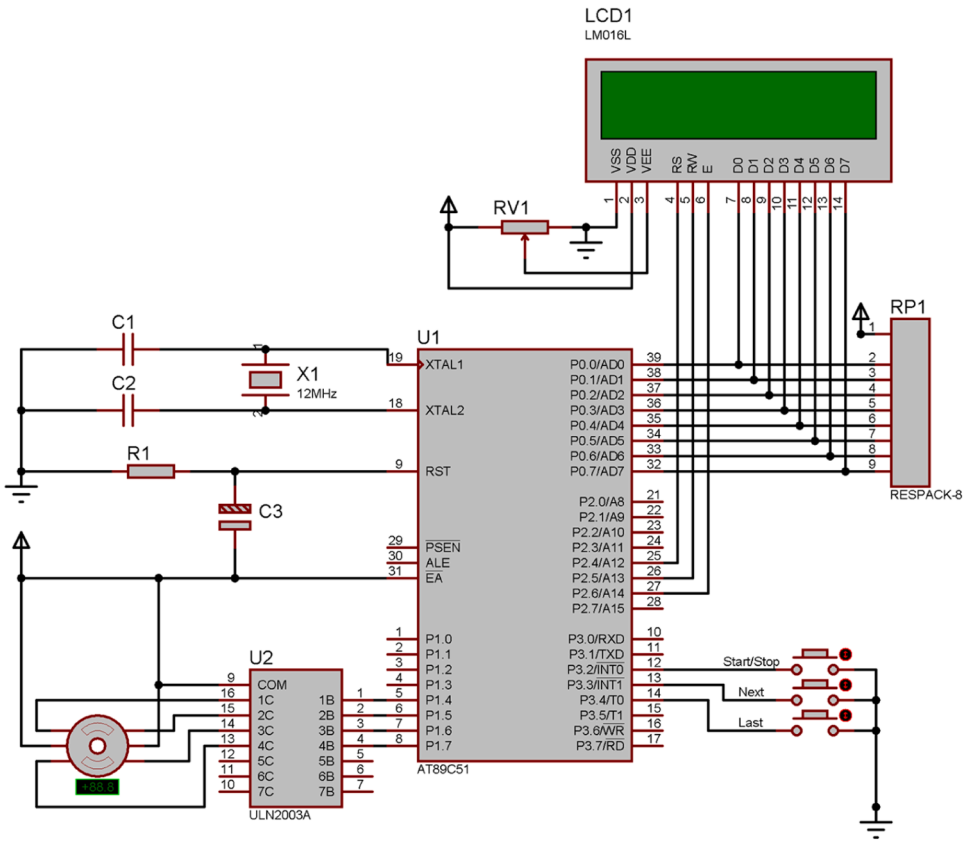

Fig. 2. Control board circuit diagram.

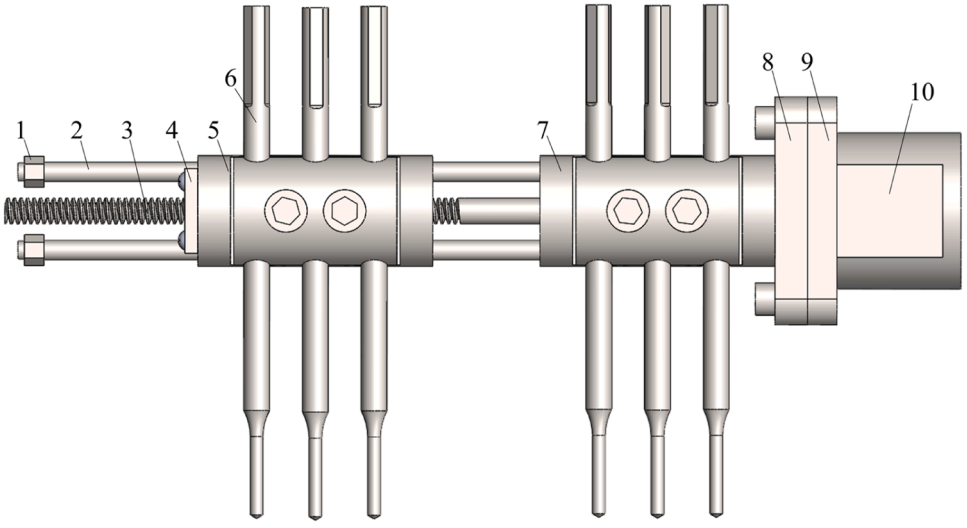

1 - Limit nut
2 - Guide Bars
3 - Lead screw
4 - Traction Flange
5 - Movable Basement
6 - Bone Screws
7 - Fixed Basement
8 - Junction Plate (for basement)
9 - Fixed Plate (for motor)
10 - Declaration Stepper Motor

Fig. 3. Schematic representation of the ACDO mechanical device.

to the lead screw by the thread can translate in the axial direction along the lead screw. The traction flange is fixed on a movable basement (5), which is used to fix the bone screws (6). A fixed and a movable basement are used to sustain the reactive force produced by the DF. With the movement of the movable basement, the BS fastened to the bone screws can be separated. Two guiding bars (2) are used to limit the translational trajectory, which causes the movable basement to slide smoothly on it and maintains the linearity of the DV. Two limit nuts (1) were installed at the ends of the guiding bars to limit the maximum distraction length. The approximate design parameters of the key components are shown in Table 1.

A deceleration stepper motor (hereinafter referred to as motor) (20BYJ46–077, manufactured by Shenzhen Maintex Intelligent Control CO.,LTD, Shenzhen City, China) is used in the experimental prototype. By driving the motor to rotate at a specific speed for a specific duration, the movable basement can translate and position precisely according to the DO process. A precise control system is implemented in the control board to actuate the motor and control the angular position of the motor shaft. By alternately energizing the phase windings of the stepper motor, the rotator can rotate in the stator. Based on this mechanism, the motor is controlled by controlling the parameters in the energization process, including the energization sequence, energization interval, and total energization time, which are related to the direction, speed, and time of rotation, respectively. Table 2 lists the specifications of the motor.

The motor shaft was inserted into the lead screw, with a 1-mm lead, 1-mm pitch, trapezoidal thread, and length of 115 mm including a 50 mm thread section. Through a nonrotational body, the entire driving rotation of the motor can be transmitted to the lead screw simultaneously. Based on previous research on DO and the related surgical experience, the required DF for an LLR surgery is 120 N [31–33]. In the proposed mode of the ACDO process (discussed in Section 2.1), the output thrust can theoretically reach 200 N continuously and stably calculated by Eq. (3) with the detent torque of the motor, which makes it possible to pull the BS smoothly and continuously. Using the specifications of the motor, lead-screw mechanism, and actuator in the control board, the theoretical movement and positioning accuracy of the device can be evaluated and calculated. The microcontroller can energize the motor in the four-phase, eight-beat mode, which causes the rotator of the motor to rotate at a step angle of 7.5°. A gearbox with a reduction ratio of 1/85 was integrated into the motor; thus, the step angle of the output shaft was 0.088°. This device can control the distraction process with maximum movement and positioning accuracy of ± 0.24 μm. The micro-stepping control mode of the actuator can further improve the accuracy while causing cost-to-torque instability, which may shut down the motor. Based on comprehensive considerations of surgical objects (long bones), a lower but sufficient accuracy was chosen in exchange for working stability. Fig. 4 presents the linear DV of the device.

As shown in Fig. 4, two sets of bone screws fixed with two basements should be drilled and connected to the treatment area on either side of the osteotomy point. The movable basement should be connected to the BS away from the trunk, thereby pulling the BS to the expected position. The fixed basement is connected to another BS as a locator to ensure that the relative distance between the two bone segments is maintained.

Table 1
Design parameters of the key components.

Components	Design parameters	
Lead-screw	Thread Pitch	1 mm
	Screw diameter	4 mm
	Screw length	115 mm
	Thread length	70 mm
Traction flange	Length	13 mm
	Width	13 mm
	Thickness	5 mm
Basement	Length	36 mm
	Width	17 mm
	Height	25.5 mm
Guiding bar	Diameter	3 mm
	Length	116 mm

Table 2
Specifications of the deceleration stepper motor (20BYJ46–077).

20BYJ46–077 motor			
Rated Voltage	5 V DC	Phase	4
Reduction Ratio	1/85	Step Angle	7.5°
Pull-in Torque	$\geq$ 40mN·m	Friction Torque	39.2–196mN·m
Detent Torque	$\geq$ 60mN·m	Exciting Method	1–2
Temp Rise	$\leq$ 60K	Noise	$\leq$ 40dB
DC Resistance	22Ω ± 10%	Insulation Resistance	$\geq$ 50MΩ500VDC

During the design process of the ACDO device, the dimensions of each section are minimized to ensure portability under the premise of meeting the strength and design requirements, which are stipulated in the mechanical design manual, including the requirements of size design and strength check (axial force acting on the screw). Another factor that prevents ACDO devices from being used is their weight. The target weight of the device is less than 200 g. Through mechanical analysis and strength considerations, different types of materials are chosen for manufacturing different sections by considering the weight and strength requirements. Magnesium–aluminium alloy 7075 and 6061 are respectively used to manufacture the basement and connection section to reduce their weights; stainless steel 316 and 304 are respectively used to manufacture the transmission section and guiding bar to ensure distraction linearity and stability. The magnesium–aluminium alloy (Lv Tai Industrial CO.,LTD, Changsha City, China) is lightweight and possesses sufficient mechanical properties for the basement and connection section resisting the horizontal force of 200 N from the bone screws, and stainless steel (Yu Ding Sheng Metals CO.,LTD, Foshan City, China) possesses the advantages of high strength and high corrosion resistance. In this study, the weight of the entire device was 146 g, comprising the guiding section of 13.14 g, transmission section of 13.64 g, basements of 60.74 g, connection section of 8.30 g, six bone screws of 22.26 g, and several screws, which can reduce its impact on daily life.

A distance-measuring section, which is composed of a capacitive grid sensor and its control circuit, is added to the system for noncontact measurement of the distraction length. The capacitive grid sensor consists of two main components: a moving grid and a stationary grid that are parallel to each other. The moving grid is pasted on the movable basement, whereas the stationary grid is pasted on the guiding bar. With the movement of the moving grid on the stationary grid, the coupling area between them changes gradually, causing changes in the capacitance. Therefore, the above process occurs as the basement slides on the guiding bar. The control circuit, which is integrated into a calculating board (a printed circuit board for the distance measuring system), is designed to convert the change in capacitance into displacement. This circuit consists of the LCD, microcontroller, and operational amplifier. The control board can obtain the distraction length, display it on the LCD, and upload it to the data cloud using the Bluetooth module. Fig. 5 illustrates the capacitive grid sensor and block diagram of the calculation circuit modules.

Based on the modelling results and theoretical analysis, under the empty-load condition, the general characteristics of the proposed ACDO device are estimated, as shown in Table 3. The detailed experimental values are presented in Section 3.

2.1. Experimental setup

Fig. 6 shows the prototype of the proposed ACDO distractor for LLR with its preliminary control board and a portable power bank of 5 V DC. Four buttons were added to the circuit of the preliminary control board to control the rotational speed and direction of the motor, thereby facilitating the prototype experiment. An experimental simulation was

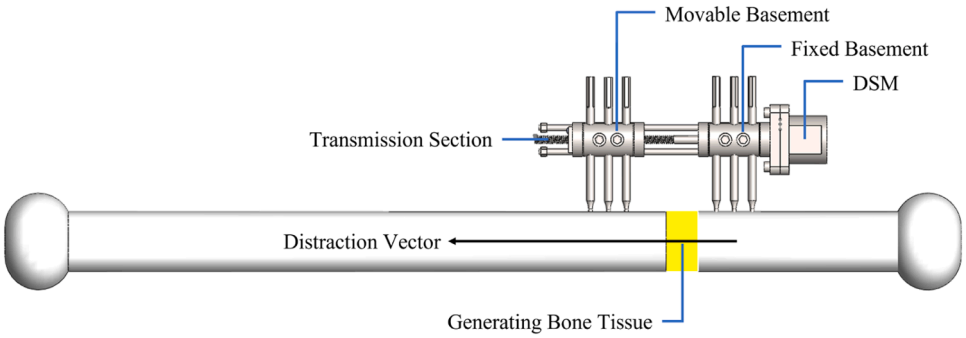

Fig. 4. Schematic illustration of linear DV of the device.

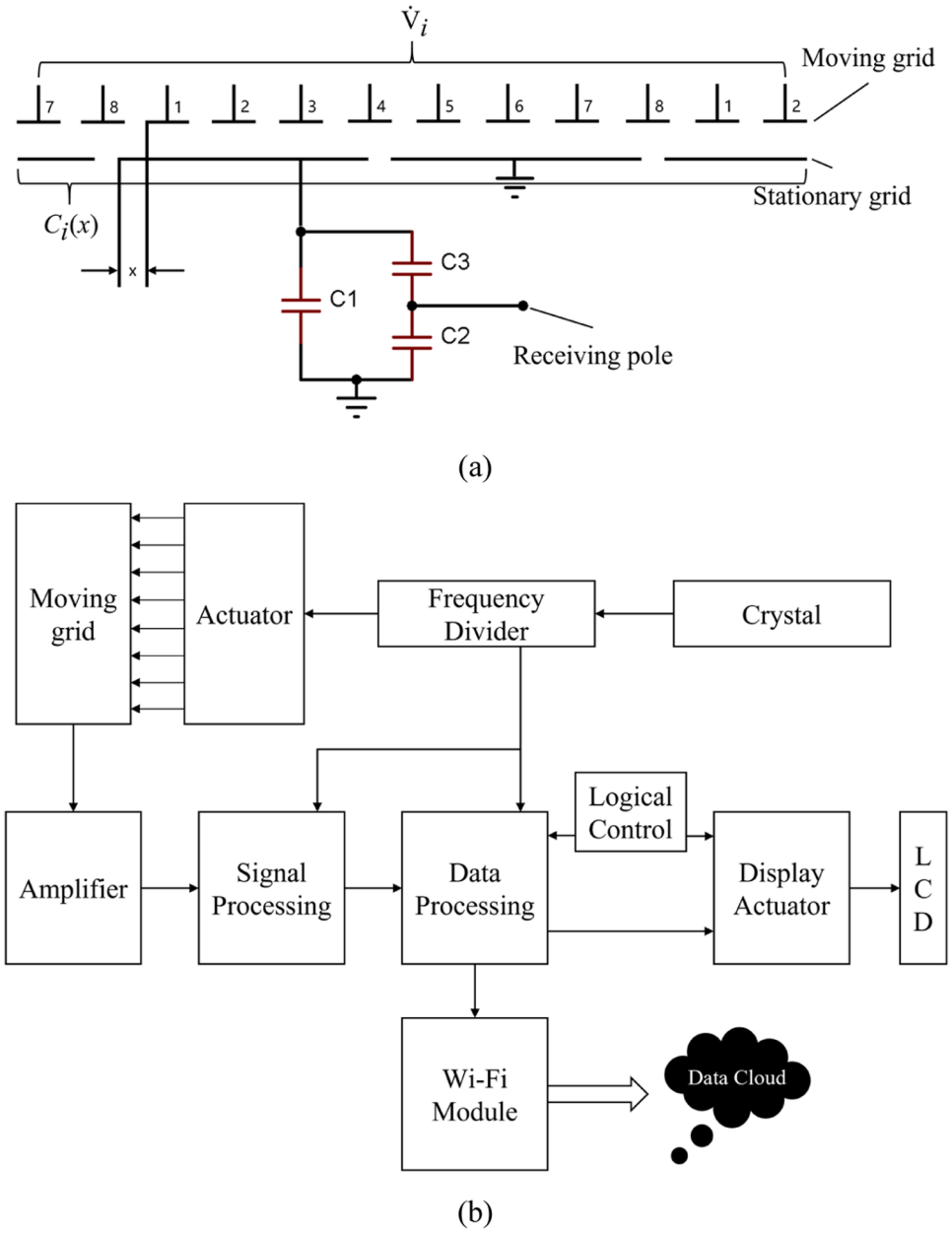

Fig. 5. Schematic diagram of the noncontact measurement system: (a) equivalent circuit diagram of the capacitive grid sensor and (b) block diagram of the calculation circuit modules.

Table 3
General characteristics of the proposed ACDO device.

Total size (mm)	Maximum travel (mm)	Generated force (N)	Distraction rate (mm/min)	Distraction accuracy (μm)	Distraction step error (μm)
146	50	≈200	0.2~10	0.24	0.002

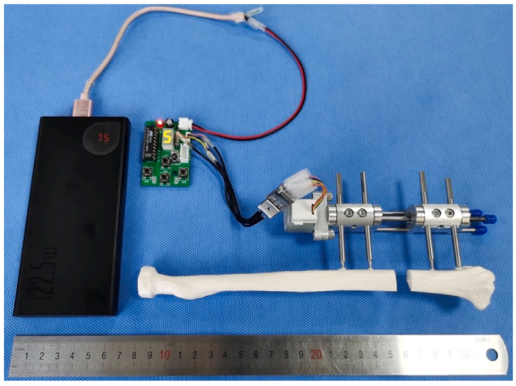

Fig. 6. Prototype of the proposed ACDO distractor. Two synthetic BS are used to simulate the performance of the ACDO surgery.

conducted to evaluate the device performance. Several previous studies have shown that a standard DO protocol for LLR requires the following working parameters: distraction length: 10–20 mm; DR: 0.5–2 mm/day; DF: ≈120 N [34–36]. In addition to the general DO parameters, a new distraction condition to be studied is proposed and can be implemented in the prototype, which is named as accordion manoeuvre [37]. In contrast to the common distraction process, which is unidirectional and single stroke, an alternate cyclic distraction-compression (CDC, or named as accordion manoeuvre) are used to replace the traditional distraction process. Each CDC contains a distraction process and compression process, and the ACDO process consists of *n* repeated CDC.

During preliminary testing of the control board, the stepless rate of movement basement in the range of 0.2–5 mm/min, distraction lengths in the range of 0–50 mm, and dynamizing frequencies in the range of 0–20 times were reached. To estimate the optimal distraction mode in LLR at different regions of the body, and prepare for further biological experiments, some common values of the DO parameters (DRs: 1.0, 0.5, and 0.25 mm/min; distraction length: 10 mm; CDC: 0, 5, and 10 times) were chosen and combined into nine distraction modes (the distraction length was chosen as 10 mm to reduce repetitive work). These modes are presented in Table 4; the theoretical distraction time was calculated and

Table 4
Predetermined parameters of the nine treatment modes.

Mode	DR (mm/min)	DL (mm)	CDC (times)	DT (min)	Description
M.1	1.00	10.0	0	12.5	High DR - Low CDC
M.2	1.00	10.0	5	25.0	High DR - Mid CDC
M.3	1.00	10.0	10	40.0	High DR - High CDC
M.4	0.50	10.0	0	22.5	Mid DR - Low CDC
M.5	0.50	10.0	5	45.0	Mid DR - Mid CDC
M.6	0.50	10.0	10	70.0	Mid DR - High CDC
M.7	0.25	10.0	0	42.5	Low DR - Low CDC
M.8	0.25	10.0	5	85.0	Low DR - Mid CDC
M.9	0.25	10.0	10	130.0	Low DR - High CDC

(DL: distraction length, DT: distraction time).

timed continuously during the experiment, and it could be suspended in the actual treatment. Fig. 7 illustrates the proposed distraction modes. A rest time of 0.5 min was added to the distraction process (Fig. 7). The standard testing environment was as follows: an atmospheric pressure of approximately 100.7 kPa and a room temperature of 25 C.

In the physical simulation, a SANLIANG digital calliper with a resolution and precision of 0.01 mm was used to measure the distraction length for comparison with the proposed distance-measuring system. A SANLIANG NK-200 N force gauge with a resolution of 1 N was used to measure the generated DF. For testing the operation stability, position error, and expected generated force, the experiment was conducted under the applied loading condition to determine the feasibility and error range of the control and calculation circuits. The designed testing parameters were used to assess the results of the DO process and for a comparison in repeated experiments to evaluate the repeatability of the system. Subsequently, the experimental results were presented as line graphs generated using IBM SPSS.

3. Results

3.1. Accuracy experiment

We mainly observed the running stability and determined the translational and positional accuracy, which were evaluated using mean relative errors. The preliminary control board can drive the motor with a minimal response time of 2 ms and an extremely low step error. During the experiment, the rotation of the lead screw and translation of the movable basement were stable and continuous without any transient breakdown or fault. The no-load running experiment proved that the linear DV and expected distraction length were smooth and accurate, respectively. After the experiment, we assessed the precision of our linear motion system (a screw–nut mechanism) by calculating the relative errors of the DO parameters between the theoretical and measured values in repeated measurements. Table 5 presents the results of the data analysis and evaluation.These results indicate that the proposed mechanical device is capable of generating a precise distraction process and an extremely low empty travel during the contraction process. The lead screw with the trapezoidal thread exhibited excellent self-locking performance. In the stationary state of the experiment, the movable basement was stable and capable of resisting tremendous force.

3.2. Physical experiment

An external thrust was applied to the movable basement of the device to test the continuous DF generated by the motor and screw–nut mechanisms. As shown in Table 2, the theoretical thrust generated by the screw–nut mechanism is approximately 200 N. In the experiment, the device was fixed to a specially designed carriage. The pull/pressure side of the force gauge was pressed onto the traction flange, and the other side was pressed against the wall. Hence, the entire force measurement system was fixed at both ends, and only the traction flange could translate and push the pressure head of the force gauge. The force gauge indicated that the pressure could reach 198 N. Hereafter, distinct vibrations and heating occurred at the movable basement and the motor, respectively. The optimal generated DF of the proposed device was 0–150 N. According to previous research [31–33], as well as the existing manual distractor, the magnitude of the required force is approximately 120 N in the LLR. Therefore, a generated DF of 198 N is sufficient for application in LLR surgery.

The results revealed that the positioning and translating accuracy was 0.24 μm and the maximum relative error of DR was 0.80%. In the duration limit test, the device operated for a lengthy period (69 min) without any breakdown or fault with a small amount of heating on the actuator that cannot be avoided under various distraction modes.

Our ACDO device include the function of a monolateral fixator. The sterilized mechanical device is applied during osteotomy and connected

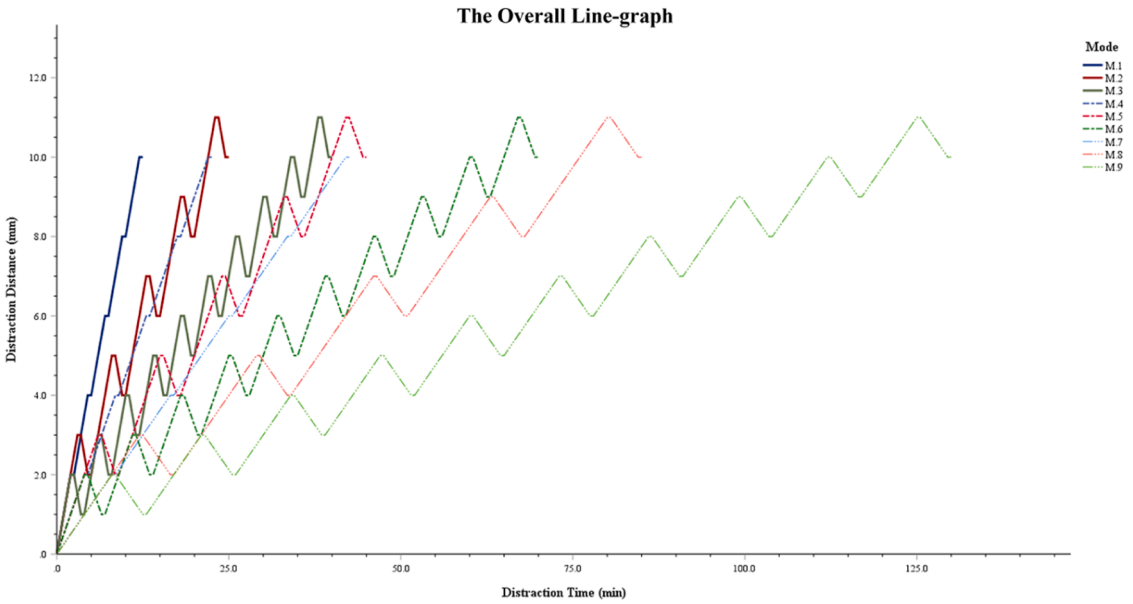

Fig. 7. Line graph of nine proposed distraction modes.

Table 5
Data analysis and evaluation.

Test	Mean measured DR (mm/min)	Mean measured DL (mm)	DR relative error (%)	DL relative error (%)
T.1	1.000	10.00	0.00	0.00
T.2	0.998	9.98	0.20	0.20
T.3	0.995	9.95	0.50	0.50
T.4	0.499	9.98	0.20	0.20
T.5	0.498	9.96	0.40	0.40
T.6	0.497	9.93	0.80	0.70
T.7	0.250	10.0	0.00	0.00
T.8	0.250	9.98	0.40	0.20
T.9	0.249	9.94	0.80	0.60

to both bone segments with half-pins. From Day 0 to the end of consolidation period, there is no need to uninstall the device, while additional control board and power are conneted to mechanical device when distraction is implemented. The monolateral fixator is an important device to achieve limb lengthening and deformity correction used in clinical settings by orthopedists. As a monolater fixator with electronic control, our ACDO device with the current size can be used for limb lengthening for human bones such as humerus, radius, ulna, etc. [38,39]. For animal experiments, our ACDO device theoretically has an axial force upper limit of 198 N, a magnitude suitable for applications such as the rabbit tibia [40]. Apart from monolateral external fixators, there are ring fixators such as Ilizarov-type and Hexapod-type being used in clinical settings. Theoretically, 3 to 6 ACDO units can be added in these systems to achieve electronic control and continuous distraction as long as the weight and cost of the system can be rationally balanced.

In comparison with other state-of-the-art automated continuous distraction devices ([22,41,42]), our distractor has a more compact shape (17 mm × 26 mm × 120 mm) to satisfy portability requirements, is more lightweight (146 g), and generates a higher output force (DFmax = 198 N) to implement in LLR ([22,41,42]). Furthermore, we developed a man–machine-interaction software to solve the problem of programming the control board, and a data cloud to facilitate the re-inspection of patients. Compared with other ACDO devices, such as those developed by Hatefi and colleagues [41,42], which have several buttons for speed adjustments, the proposed control method enables stepless speed and force control. With the matched man–computer interaction system, it is convenient to set precise distraction rate based on the diagnostic results.

4. Discussion and conclusions

Distraction osteogenesis has been used for long bone lengthening of the extremities, including the femur, tibia, humerus, and ulna (the long tubular bones of the limbs). In contrast to traditional LLR methods, this technique can provide better treatment and reduce trauma. By using an automated continuous distractor in LLR, an optimal DO process can aid in tissue healing.

In this study, an ACDO device with a matched control monitoring system for LLR was designed, programmed, and manufactured. The device is capable of generating an optimal continuous DF of 150 N with a theoretical positioning and translation accuracy of 0.24 μm. The experimental results demonstrate that the proposed device and linear control system can generate an automatic and continuous DO process with high precision (translating accuracy of 0.2–0.3 μm) and smoothness (the relative error of DR not exceeding 0.80%). This has the potential to reduce pain during DO and aid in tissue healing. With the man–machine-interaction system and the control method of controlling the parameters in the energization process, the DO process can be precisely controlled. The control system can drive the motor continuously and stably while providing a highly accurate distraction motion and a controlled and stable DF. The monitoring system can connect clinicians and patients remotely, thereby facilitating the setting and programming of the ACDO device by doctors and providing patients with the option of returning home for treatment. Compared to existing devices, the distraction rate of 0.2 mm/min is much smaller than the manual operation rate. Within 1 mm distraction distance, the proposed device can run in 300 s, while the existing device is limited to run time of a few seconds. The proposed device can generate a controlled and smooth DF to pull and position the BS appropriately for bone lengthening. The control monitoring system can enable the remote control and monitoring of patients by doctors, thereby providing the patients with a better treatment environment and a convenient re-inspection process.

However, the inconvenience caused by wiring—because the electric control box needs to be linked to the motor via a cable—can be eliminated using wireless transmission technologies, and the device can achieve better integration by customizing an integrated driver-transmission section. The duration of operation is still limited by the heating of the actuator and the volume of the motor. Due to the existing motor and actuator, the heating problem is inevitable, and it is difficult to achieve both light-weight and long-working. While this issue

represents a potentially serious limitation compared with existing manual DO devices, with further work there is scope for the proposed ACDO device and its control system to be further improved in this regard in future. In an ongoing pre-clinical study, we are assessing the clinical, radiographic, and histologic evidence of bone formation in a DO wound (lengthened 10 to 20 mm) after being operated using our ACDO device in different situations, and we are attempting to find the best situation for osteogenesis. Based on the mechanical instrumentation of the proposed ACDO device and its matched control system, we will investigate the effect of the mechanical environment on bone regeneration, find the optimal material for bone regeneration and optimize the structure of the device. With the functions and characteristics of the precise control system, the distraction rate and frequency of CDC are fully controllable. As such, the proposed technology can serve as a platform, which in future may help researchers to explore the effect of different distraction conditions on bone cell growth and remodelling, and lead to improvements in fracture healing.

Funding

This study was supported by the Beijing JST Research Funding (code: YGQ-202215).

Ethical approval

Not required

Declaration of Competing Interest

None declared.

Acknowledgements

Fanwu MENG guided the device design and manuscript preparation. Xinghua YIN provided the related instructions for the DO technique in LLR and LON surgery.

References

[1] A. Codivilla, The classic: on the means of lengthening, in the lower limbs, the muscles and tissues which are shortened through deformity 1905, Clin. Orthop. Relat. Res. 466 (2008) 2903–2909, https://doi.org/10.1007/s11999-008-0518-7.
[2] G.A. Ilizarov, The principles of the Ilizarov method, Bull. Hosp. Jt. Dis. Orthop. Inst. 48 (1988) 1–11.
[3] G.A. Ilizarov, The tension-stress effect on the genesis and growth of tissues: part II The influence of the rate and frequency of distraction, Clin. Orthop. Relat. Res. 239 (1989) 263–285.
[4] G.A. Ilizarov, The tension-stress effect on the genesis and growth of tissues. Part I. The influence of stability of fixation and soft-tissue preservation, Clin. Orthop. Relat. Res. 238 (1989) 249–281.
[5] G.A. Ilizarov, Clinical application of the tension-stress effect for limb lengthening, Clin. Orthop. Relat. Res. 250 (1990) 8–26.
[6] A. Aykan, et al., Mandibular distraction osteogenesis with newly designed electromechanical distractor, J. Craniofac. Surg. 25 (2014) 1519–1523, https://doi.org/10.1097/scs.0000000000000922.
[7] M.M. Mofid, et al., Craniofacial distraction osteogenesis: a review of 3278 cases, Plast. Reconstr. Surg. 108 (2001) 1103–1114, https://doi.org/10.1097/00006534-200110000-00001 (discussion 1115–7).
[8] F. Molina, Mandibular distraction osteogenesis: a clinical experience of the last 17 years, J. Craniofac. Surg. 20 (2009) 1794–1800, https://doi.org/10.1097/scs.0b013e3181b5d4de.
[9] M.J. Troulis, L.B. Kaban, Complications of mandibular distraction osteogenesis, Oral Maxillofac. Surg. Clin. North Am. 15 (2003) 251–264, https://doi.org/10.1097/scs.0b013e3181ecc6e5.
[10] B.R. Goldwaser, M.E. Papadaki, L.B. Kaban, et al., Automated continuous mandibular distraction osteogenesis: review of the literature, J. Oral Maxillofac. Surg. 70 (2012) 407–416, https://doi.org/10.1016/j.joms.2011.01.042.
[11] J.T. Park, et al., A piezoelectric motor-based microactuator-generated distractor for continuous jaw bone distraction, J. Craniofacial. Surg. 22 (2011) 1486–1488, https://doi.org/10.1097/scs.0b013e31821d196b.
[12] U.M. Djasim, et al., Continuous versus discontinuous distraction: evaluation of bone regenerate following various rhythms of distraction, J. Oral Maxillofac. Surg. 67 (2009) 818–826, https://doi.org/10.1016/j.joms.2008.08.016.
[13] L.W. Zheng, L. Ma, L.K. Cheung, Angiogenesis is enhanced by continuous traction in rabbit mandibular distraction osteogenesis, J. Cranio-Maxillofacial Surg. 37 (2009) 405–411, https://doi.org/10.1016/j.jcms.2009.03.007.
[14] S. Hatefi, M. Etemadi Sh, Y. Yihun, R. Mansouri, A. Akhlaghi, Continuous distraction osteogenesis device with MAAC controller for mandibular reconstruction applications, Biomed. Eng. Online 18 (2019) 43, https://doi.org/10.1186/s12938-019-0655-0.
[15] A. Aykan, et al., Mandibular distraction osteogenesis with newly designed electromechanical distractor, J Craniofacial Surg 25 (2014) 1519–1523, https://doi.org/10.1097/scs.0000000000000922.
[16] S. Dundar, et al., Comparison of the effects of local and systemic zoledronic acid application on mandibular distraction osteogenesis, J. Craniofacial Surg. 28 (2017) e621–e625, https://doi.org/10.1097/scs.0000000000003629.
[17] L. Zheng, et al., High-rhythm automatic driver for bone traction: an experimental study in rabbits, Int. J. Oral Maxillofac. Surg. 37 (2008) 736–740, https://doi.org/10.1016/j.ijom.2008.03.005.
[18] M. Chung, et al., An implantable battery system for a continuous automatic distraction device for mandibular distraction osteogenesis, J. Med. Dev. 4 (2010), 045005, https://doi.org/10.1115/1.4003007.
[19] N.B. Crane, et al., Design and feasibility testing of a novel device for automatic distraction osteogenesis of the mandible, in: Proceedings of the ASME 2004 International Design Engineering Technical Conferences and Computers and Information in Engineering Conference. Volume 2: 28th Biennial Mechanisms and Robotics Conference, Parts A and B. Salt Lake City, Utah, USA, 2004, pp. 611–620, https://doi.org/10.1115/DETC2004-57232. September 28–October 2, ASME.
[20] F. Savoldi, et al., The biomechanical properties of human craniofacial sutures and relevant variables in sutural distraction osteogenesis: a critical review, Tissue Eng. 24 (2017) 225–236, https://doi.org/10.1089/ten.teb.2017.0116.
[21] N. Meyers, et al., Novel systems for the application of isolated tensile, compressive, and shearing stimulation of distraction callus tissue, PLoS One 12 (2017), e0189432, https://doi.org/10.1371/journal.pone.0189432.
[22] J. Wiltfang, et al., Continuous and intermittent bone distraction using a microhydraulic cylinder: an experimental study in minipigs, Br. J. Oral Maxillofac. Surg. 39 (2001) 2–7, https://doi.org/10.1054/bjom.2000.0564.
[23] J.C. Magill, et al., Automating skeletal expansion: an implant for distraction osteogenesis of the mandible, J. Med. Dev. 3 (2009), 014502, https://doi.org/10.1115/1.3071969.
[24] A. Ayoub, W. Richardson, A new device for micro incremental automatic distraction osteogenesis, Br. J. Oral Maxillofac. Surg. 39 (2001) 353–355, https://doi.org/10.1054/bjom.2000.0659.
[25] M.M. Mofid, et al., Spring-mediated mandibular distraction osteogenesis, J. Craniofacial Surg. 14 (2003) 756–762, https://doi.org/10.1097/00001665-200309000-00029.
[26] H.Z. Zhou, et al., Transport distraction osteogenesis using nitinol spring: an exploration in canine mandible, J. Craniofacial Surg. 17 (2006) 943–949, https://doi.org/10.1097/01.scs.0000236437.74850.26.
[27] K. Yamauchi, et al., Timed-release system for periosteal expansion osteogenesis using NiTi mesh and absorbable material in the rabbit calvaria, J. Cranio-Maxillofacial Surg. 44 (2016) 1366–1372, https://doi.org/10.1016/j.jcms.2016.06.015.
[28] S. Idelsohn, et al., Continuous mandibular distraction osteogenesis using superelastic shape memory alloy (SMA), J. Mater. Sci. Mater. Med. 15 (2004) 541–546, https://doi.org/10.1023/b:jmsm.0000021135.72288.8f.
[29] J. Wee, et al., Development of a force-driven distractor for distraction osteogenesis, J. Med. Dev. 5 (2011), 041004, https://doi.org/10.1115/1.4005321.
[30] H. Shahrokh, et al., Review of automatic continuous distraction osteogenesis devices for mandibular reconstruction applications, Biomed. Eng. Online 19 (1) (2020) 17, https://doi.org/10.1186/s12938-020-00761-8, 1 Apr.
[31] L. David, et al., Rabbit knee joint biomechanics: motion analysis and modeling of forces during hopping, J. Orthop. Res. 23 (2005) 735–742. http://doi.org/10.1016/j.orthres.2005.01.00.
[32] J. Mora-Macías, et al., Distraction osteogenesis device to estimate the axial stiffness of the callus in vivo, Med. Eng. Phys. 37 (2015) 969–978, https://doi.org/10.1016/j.medengphy.2015.07.008.
[33] H. Konstantin, et al., The role of soft-tissue traction forces in bone segment transport for callus distraction, Strat. Traum Limb. Recon. 10 (2015) 21–26. http://doi.org/10.1007/s11751-015-0220-8.
[34] Ouyang, et al., Distraction osteogenesis and arthrodesis as a new surgical option for chondrosarcoma in the distal tibia, World J. Surg. Oncol. 13 (2015) 187. http://doi.org/10.1186/s12957-015-0604-8.
[35] T.M. Chappell, et al., Distal tibial distraction osteogenesis – an alternative approach to addressing limb length discrepancy with concurrent hindfoot and ankle reconstruction, J. Orthopaedic Surg. Res. 14 (2019) 244, https://doi.org/10.1186/s13018-019-1264-0.
[36] A. Ali, et al., Unprecedented tibial bone lengthening of 33.5cm by distraction osteogenesis for the reconstruction of a subtotal tibial bone defect. A case report and literature review, BMC Musculoskelet. Disord. 22 (2021) 88, https://doi.org/10.1186/s12891-021-03950-1.
[37] Makhdom A.M., Cartaleanu A.S., Rendon J.S., et al. The accordion maneuver: a noninvasive strategy for absent or delayed callus formation in cases of limb lengthening. 2015: 912790. 10.1155/2015/912790.
[38] A.Y Pawar, et al., Does humeral lengthening with a monolateral frame improve function? Clin. Orthop. Relat. Res. 471 (1) (2013) 277–283, https://doi.org/10.1007/s11999-012-2543-9.

[39] K. Mader, et al., Shortening and deformity of radius and ulna in children: correction of axis and length by callus distraction, J. Pediatr. Orthop. B 12 (3) (2003) 183–191, https://doi.org/10.1097/01.bpb.0000057485.91570.e9.
[40] J. Reifenrath, et al., Axial forces and bending moments in the loaded rabbit tibia in vivo, Acta Vet. Scand. 54 (1) (2012) 21, https://doi.org/10.1186/1751-0147-54-21, 30 Mar.
[41] S. Hatefi, et al., Continuous distraction osteogenesis device with MAAC controller for mandibular reconstruction applications, Biomed. Eng. Online 18 (2019) 43, https://doi.org/10.1186/s12938-019-0655-0.
[42] S. Hatefi, et al., Automatic continuous distraction osteogenesis device for hand reconstruction applications, Med. Eng. Phys. 101 (2022), 103770, https://doi.org/10.1016/j.medengphy.2022.103770.